

Measurement of Ultrasonic Attenuation Within Regions Selected from *B*-Scan Images

KEVIN J. PARKER, MEMBER, IEEE, AND ROBERT C. WAAG, MEMBER, IEEE

Abstract—This paper describes the calculation of absolute ultrasonic attenuation as a function of frequency by processing backscattered signals obtained from a clinical imaging instrument. The signal processing steps are developed from a mathematical model of scattering in an attenuating medium with random inhomogeneities. Attenuation data are derived from the imaging system by recording amplitude-compressed ultrasonic echo waveforms along with transducer position information and time-varying gain values. The input-output characteristics of the receiver are employed to remove the effects of compression and gain. Attenuation values are calculated for selected regions within scans of two tissue phantoms and a normal breast. The values agree with other independent measurements and illustrate the requirements for incorporating quantitative attenuation measurements with clinical imaging.

INTRODUCTION

SINCE the early 1970's [1], it has been recognized that the frequency-dependent attenuation of tissues can be indicative of the presence or absence of disease states in a tissue or organ. Accordingly, frequency-dependent attenuation in tissues has been calculated from measurements of reflected, transmitted, or backscattered ultrasound and used to study abnormalities in the eye [2], indicate the development of myocardial infarcts [1], [3], [4], detect tumors [5], [6], and evaluate liver tissue [7]–[10].

Commercially available imaging systems are presently capable of a variety of dimension and volume estimates and can perform image enhancement functions, but none extract quantitative attenuation measurements. In some cases, an estimate of attenuation can be made from a *B*-scan image which shows shadowing beneath an object, such as a gallstone [11]. These effects depend, to a certain extent, on the time-varying gain selected by the clinician to boost signals returning from deeper tissues. For small attenuation differences, this qualitative approach loses the ability to discriminate tissue types.

Reliable ultrasonic attenuation measurements of tissue specimens are made difficult by phase cancellation errors [12], beam distortion effects [13], and entrapped gas [14]. However, consistent *in vitro* measurements of attenuation as a function of frequency can be obtained by carefully eliminating the sources of artifact [13]. There are additional difficulties to overcome in measurements of ultrasonic attenuation *in vivo*. The lack of sufficient through-transmission paths in abdominal

Manuscript received October 7, 1982; revised March 14, 1983. This work was supported in part by the National Science Foundation under Grant ECS 80-17683 and by the National Institutes of Health under Grant GM 09933.

The authors are with the Department of Electrical Engineering, University of Rochester, Rochester, NY 14627.

organs severely restricts the use of radiation force techniques [15], time delay spectrometry [16], and transmission reconstruction tomography [6]. The absence of plane specular reflectors within internal organs creates uncertainties in the use of nonstatistical reflection-based techniques [1], [17], [18].

The incorporation of attenuation measurements into an imaging system is also hindered by the inclusion of a compression amplifier and time-varying gain which are used to display the wide dynamic range of returning echoes and compensate for signal attenuation as a function of range. Compression effects and time-varying gain are often subjectively varied case-by-case by the clinician to improve the quality of the resulting image. Therefore, in order to obtain absolute attenuation measurements, both the nonlinear compression and instantaneous value of the time-varying gain must be taken into account.

In general, the statistical nature of backscattered ultrasonic signals from inhomogeneities or nonspecular reflectors must be considered to calculate frequency dependent attenuation of internal organs *in vivo*. Pioneering work with statistical methods in this area was carried out by Kuc and Schwartz [7], [8] who determined the slope of attenuation assuming a linear frequency dependence. In this paper, a different statistical approach has been used to determine the absolute values of attenuation as a function of frequency, thereby determining the slope of attenuation as well. No *a priori* requirement of linear frequency dependence is required. Although more work is required to define practical resolution and accuracy limits of this technique for clinical use, the preliminary results are very encouraging.

THEORY

Our calculation of frequency-dependent attenuation is based on a mathematical model which characterizes scattering as arising from random small scale fluctuations in acoustic properties of a medium. When a sample volume of the medium is irradiated by a plane wave ultrasonic signal, the scattered pressure at any point in the far field becomes a random variable. There is a well-known Fourier transform relationship between the ensemble average of the pressure squared (or intensity) and the correlation function of the variations in the material [19], [20].

Backscattered signals, which are used to create images, represent a particular case of this general theory. In a non-attenuating medium with small, zero mean fluctuations in sound speed, we designate k_0 as the average material wave-

number and $\gamma(r')$ as the zero mean sound speed fluctuations as a function of position r' . Then the complex backscattered pressure from a narrow-band signal can be written using a small scattering assumption as [20]-[22]

$$p_{bs}(r) = \frac{A}{r} \int_{v'} e^{j2k_0 n \cdot r'} \gamma(r') dv' \quad (1)$$

where A is a complex factor dependent on frequency, medium density, and amplitude of the incident wave; r is the distance between the receiver and the scattering region; v' represents the sample volume of integration; and n is a unit vector pointing in the direction of the incident sound propagation. In this expression, $p_{bs}(r)$ represents the pressure at a point. However, we assume that the output voltage from our finite area transducer is directly proportional to this pressure.

Each sample function for backscattered pressure $p_{bs}(r)$ will depend on the particular random variations in $\gamma(r')$ and, given our assumption that γ is a zero mean quantity, $p_{bs}(r)$ has a mean value of zero. However, the magnitude of backscattered pressure has a nonzero mean which can be employed to extract frequency dependent attenuation.

The effects of attenuation may be included by adding an imaginary component α to the wavenumber. Under the assumptions that $k_0 \gg \alpha$, and that $e^{-\alpha r'} \cong 1$ within the sample volume of integration, the complex backscattered pressure becomes [20]

$$p_{bs}(r) = e^{-\alpha r} \frac{A}{r} \int_{v'} e^{j2k_0 n \cdot r'} \gamma(r') dv'. \quad (2)$$

This expression is similar to the nonattenuating case, with the exception of the exponential decay term outside the integral. Thus, under weak scattering and weak attenuating assumptions, the effects of backscattering and attenuation are separable.

For a plane wave propagating through an attenuating medium, the incident wave amplitude at distance r is given in terms of its initial value p_0 by [27]

$$p_i(r) = p_0 e^{-\alpha r}. \quad (3)$$

The complex coefficient A in (2) includes the magnitude of the incident wave, so to incorporate the r dependence explicitly, we write

$$A = A(r) = A_0 e^{-\alpha r} \quad (4)$$

and (2) becomes

$$p_{bs}(r) = \frac{e^{-2\alpha r} A_0}{r} \int_{v'} e^{j2k_0 n \cdot r'} \gamma(r') dv'. \quad (5)$$

If the attenuating medium is separated from the transducer by a long water path, the distance can be rewritten as

$$r = r_0 + d \quad (6)$$

where r_0 is the distance in water from the transmitter to the attenuating medium and d is the depth of the sample volume. Assuming no attenuation takes place in the water, (5) becomes

$$p_{bs}(d) = e^{-2\alpha d} \frac{A_0}{(r_0 + d)} \int_{v'} e^{j2k_0 n \cdot r'} \gamma(r') dv'. \quad (7)$$

The separation of the attenuation from random backscatter can be accomplished by evaluating the ensemble average of the magnitude of pressure along independent scan lines through the medium.

Using (7) we have

$$\langle |p_{bs}(d)| \rangle = \frac{e^{-2\alpha d}}{(r_0 + d)} \cdot \bar{p} \quad (8)$$

where the brackets indicate ensemble averaging of magnitude; the backscattered pressure on the left-hand side has been written as a function of depth, d ; and

$$\bar{p} = \left\langle \left| A_0 \int_{v'} e^{j2k_0 n \cdot r'} \gamma(r') dv' \right| \right\rangle. \quad (9)$$

In this expression, \bar{p} is a constant whose value depends on the statistics of the material represented by $\gamma(r')$. Equation (8) shows that the ensemble average of pressure magnitudes will decay exponentially from increasingly deep sample volumes. The exponential decay is modified by the distance term in the denominator. Although individual waveforms exhibit both random scattering and attenuation effects, the absolute value of α can be obtained from the ensemble average given in (8).

When a broad-band pulse propagates through tissue, a continuous signal is received by the transducer as backscattered energy arrives from increasingly distant range. In this case, portions of the returned signal may be windowed to select sample volumes. Fourier transformations of these data yield the magnitude of pressure in the sample volume as a function of frequency. Equation (8) can then be used at each resolvable frequency to determine the absolute values of attenuation at discrete frequencies, thus permitting the functional dependence of attenuation on frequency to be found without *a priori* assumptions of slope.

METHODS

The ultrasonic image system used in our study is the Octoson made by Ausonics, Inc., Australia. In this system, the acoustic energy is transmitted and received by eight large aperture, wide-band transducers having a center frequency which we found to be near 2.5 MHz. The transducers are arranged in an arc at the base of a deep water path chamber and are weakly focused at a range of approximately 35 cm. Ultrasonic echo signals are amplified by a wide-band receiver which has a non-linear compression characteristic and a time-varying gain. The amplified RF waveforms are sent along with positional information to both the Octoson imaging circuits and to an 8 bit, 10 MHz, A/D converter for storage in digital form and later analysis. The time-varying gain values are also digitized and stored for processing which removes gain and compression effects. This processing is accomplished by using measured input-output characteristics of the Octoson.

The measurement of the input-output characteristics employed a 2.5 MHz continuous wave signal which was injected into the receiver input. During the cycle over which ultrasound echoes are normally received, the time-varying gain was swept linearly from low to high values. The receiver output waveform was digitized and demodulated. The strength of the injected signal was varied over 96 dB in 6 dB increments. The

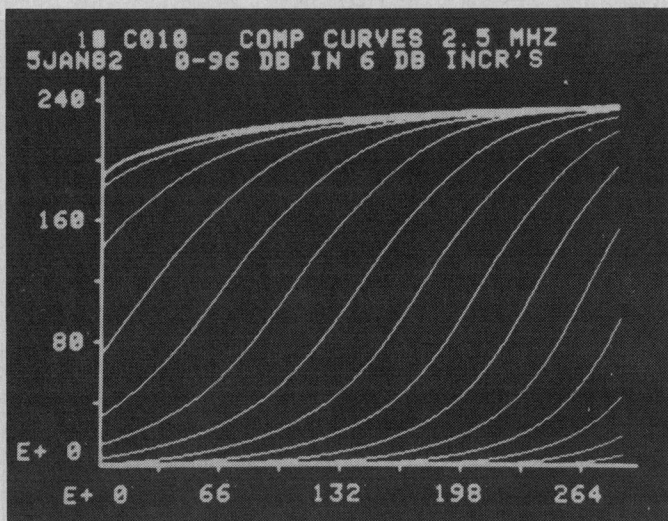


Fig. 1. Receiver input-output characteristics. Values of the output detected signal amplitude (relative linear scale) are plotted vertically as a function of time-varying gain (arbitrary units) for 17 levels of 2.5 MHz input amplitudes spanning a 96 dB range in 6 dB increments.

resulting family of waveforms is displayed in Fig. 1. The sigmoid shape of any individual curve is due to compression effects acting on an increasingly amplified signal. From these data, a table was created to map any given compressed signal amplitude into a corresponding linear value using the instantaneous value of the time-varying gain.

Two tissue phantoms were used in this study. The exact composition of these phantoms is proprietary, but independent laboratory measurements of the attenuation characteristics of the material were obtained for comparison against the estimates of the new technique. In addition, the scan of a normal female breast was processed.

First, regions 3.5 cm wide and no longer than 4.5 cm in depth were selected from *B*-scan images for processing to determine absolute attenuation. Then, 100 individual waveforms from these regions were isolated and the effects of receiver compression and time-varying gain were removed. Next, the waveforms were divided into segments of 128 data points. At a 10 MHz sampling rate, this corresponds to sample volumes of approximately 9.6 mm. In order to limit the total sample volume, a segment-to-segment overlap of 28 points was employed. An FFT routine was used with rectangular data windows to calculate the spectral magnitudes as a function of frequency and depth. Finally, the attenuation coefficient was estimated by a least square error fit of an exponential function to the mean values of backscattered pressure.

The isolated RF waveforms from the selected regions of the *B*-scan images were also demodulated and averaged to obtain a single curve of average video signal versus depth. The attenuation was calculated from this curve and ascribed to the center frequency (2.5 MHz) for comparison with the other techniques.

RESULTS

Results were obtained from a tissue-mimicking phantom made by ATS Laboratory [23]. A compound *B*-scan image of this phantom and the region selected for analysis are displayed

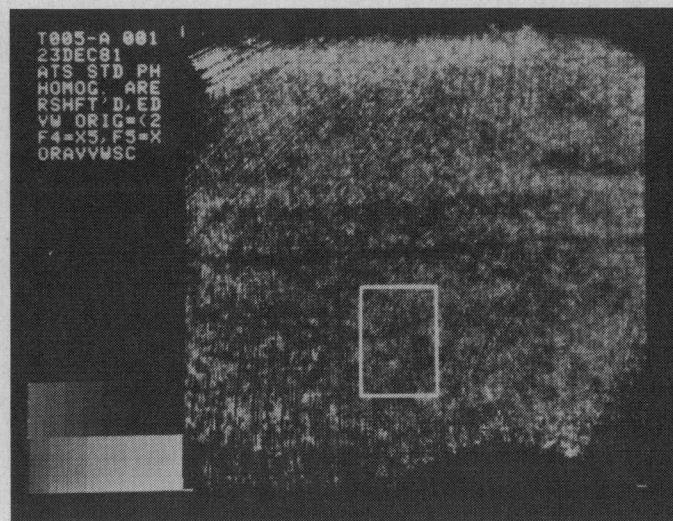


Fig. 2. ATS phantom. The rectangle indicates the region from which waveforms were selected for analysis.

in Fig. 2. Waveforms from a single transducer with a line of sight approximately parallel to the long axis of the box were employed in our calculations. The individual waveforms represent lateral shifts in the transducer line of sight. The exponential decay of 2.58 MHz (typical of other frequencies) and also the decay of the envelope are shown in Fig. 3. Attenuation values derived from the exponential decay rates are plotted versus frequency in Fig. 4 along with data found using radiation force technique.

Data were also obtained from a phantom made by Acoustic Standards Laboratory [24]. An ultrasonic image of this phantom and the region selected for analysis are displayed in Fig. 5. The exponential decay of 2.82 MHz (representative of other frequencies) as well as the decay of the envelope are shown in Fig. 6. Resulting attenuation estimates are plotted in Fig. 7 along with attenuation data measured independently [25].

Backscattered RF ultrasonic signals were also digitized during the routine clinical examination of a normal female breast. The breast image and region selected for analysis are shown in Fig. 8. Illustrative exponential decay data at 2.42 MHz are given in Fig. 9. Plots of resulting attenuation values versus frequency in Fig. 10 show a magnitude and frequency dependence consistent with values obtained by others [6], [26].

DISCUSSION

There are some features of our model that deserve comment. Although our assumption that scattering is caused by fluctuations in sound speed may be an oversimplification, a more complex model in which sound is scattered by compressibility and density variations would have the same general form as (1) but would involve a different expression for γ [19]. Since this does not enter into the frequency or range relations that we develop, our model which expresses scattering in terms of variations in sound speed is also applicable to scattering caused by fluctuations in compressibility and density.

Our model presumes that the basic statistical properties of the scattering medium do not change over the entire range

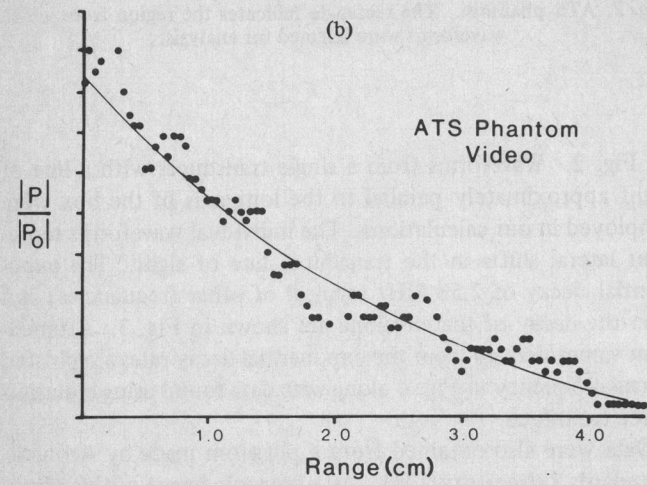
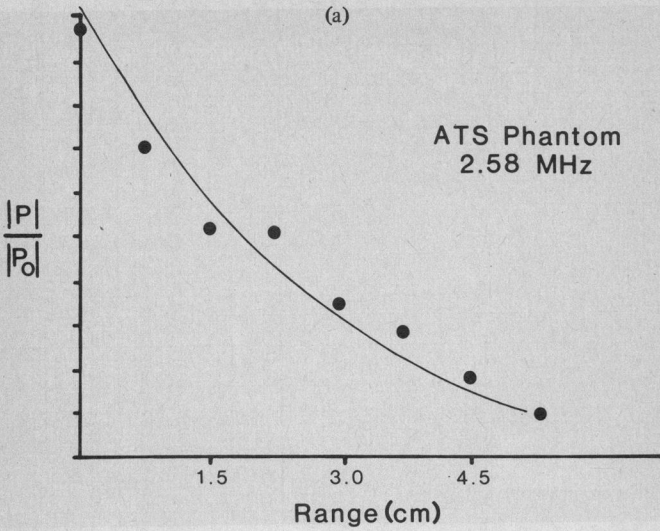


Fig. 3. Average pressure magnitude versus range in the ATS phantom (normalized vertical scale). (a) 2.58 MHz data. (b) Video signal. (● = average pressure magnitude, — = fitted exponential.)

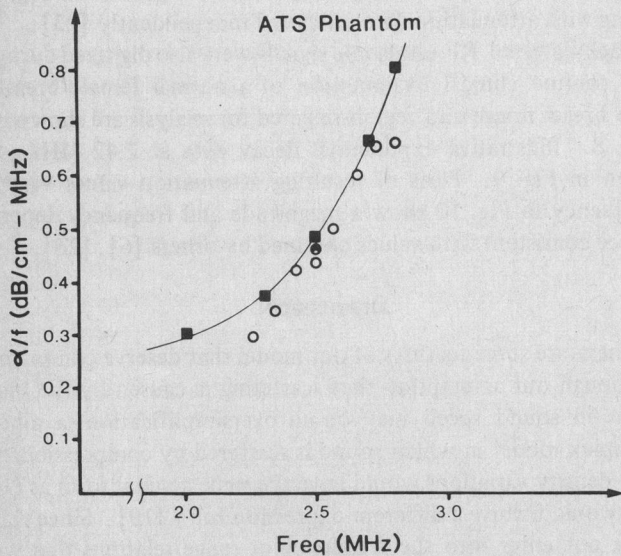


Fig. 4. Absolute attenuation versus frequency for the ATS phantom. (○ = calculated from the decay of pressure at discrete frequencies, ⊗ = calculated using the signal envelope, ■ = measured using radiation force.)

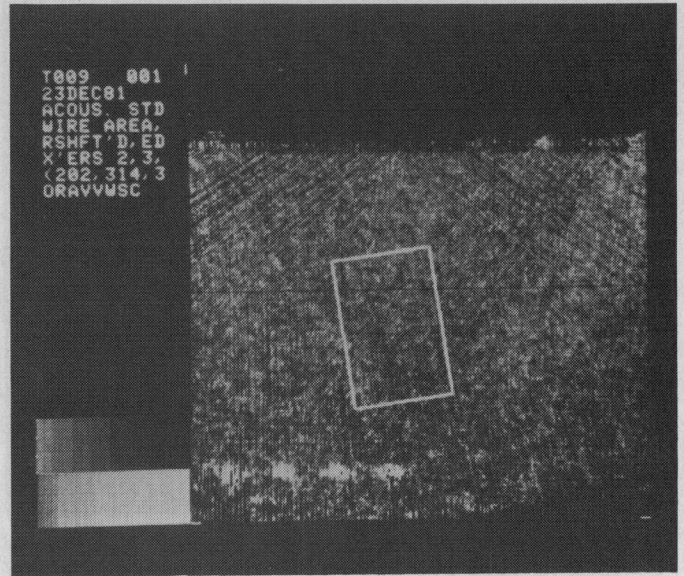


Fig. 5. Acoustic Standards phantom. The rectangle indicates the region from which waveforms were selected for analysis.

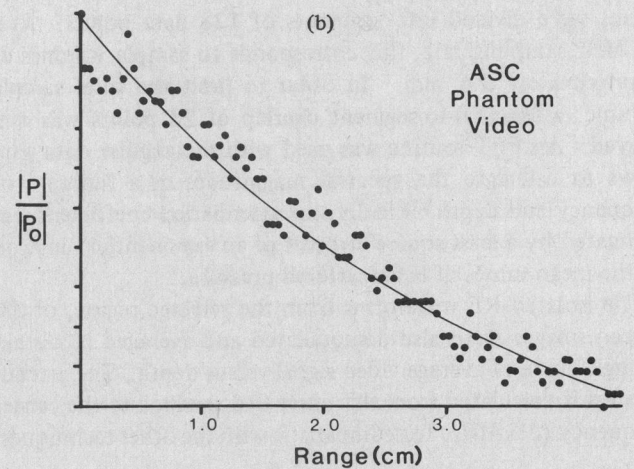
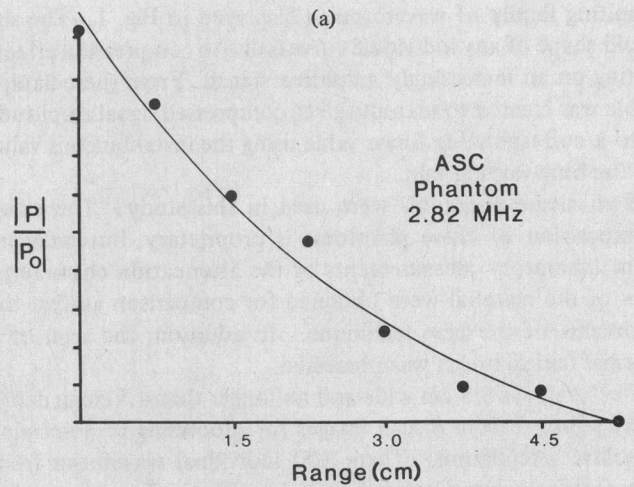


Fig. 6. Average pressure magnitude versus range in the Acoustic Standards phantom (normalized vertical scale). (a) 2.82 MHz data. (b) Video signal. (● = average pressure magnitude, — = fitted exponential.)

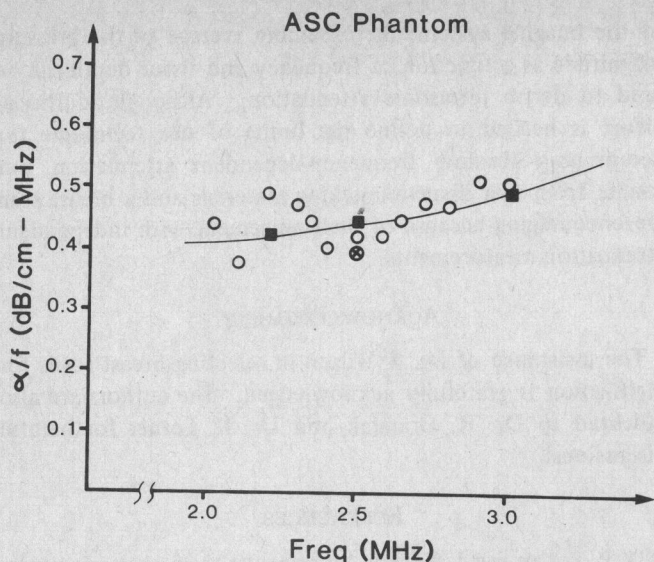


Fig. 7. Absolute attenuation versus frequency for the Acoustic Standards phantom. (O = calculated from the decay of pressure at discrete frequencies, ⊗ = calculated using the signal envelope, ■ = reference measurement of $\alpha = 0.32f^{1.38}$.)

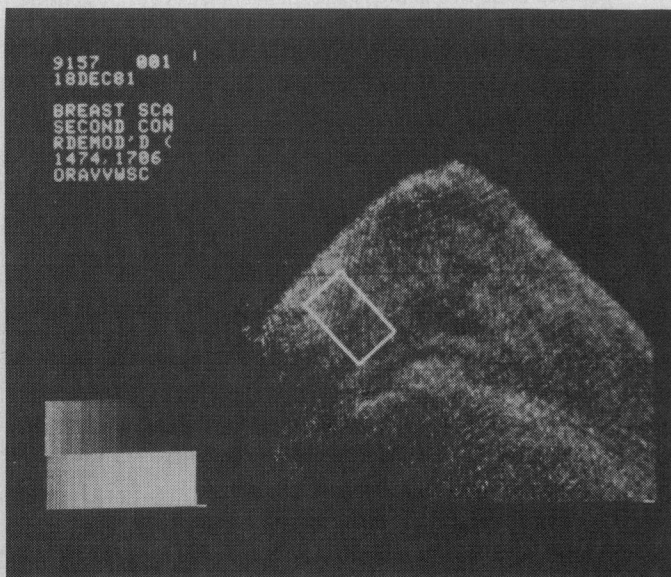


Fig. 8. Normal breast. The rectangle indicates the region from which waveforms were selected for analysis.

interval being analyzed. For example, it would be inappropriate to choose a region comprised of both medulla and cortex in the kidney. While this limits the organs or regions that may be studied with our approach, our methods can be applied to a variety of important organs such as the breast and liver which are usually sufficiently large and which sometimes contain diffusely distributed diseases.

In backscatter experiments, the transmitted pressure will vary with depth not only due to attenuation, but also by the effects of beam spreading or convergence caused by focusing. However, changes in beamwidth due to focusing were neglected over the ranges we analyzed because these ranges were a small fraction of the normalized distance from the transducer. Also

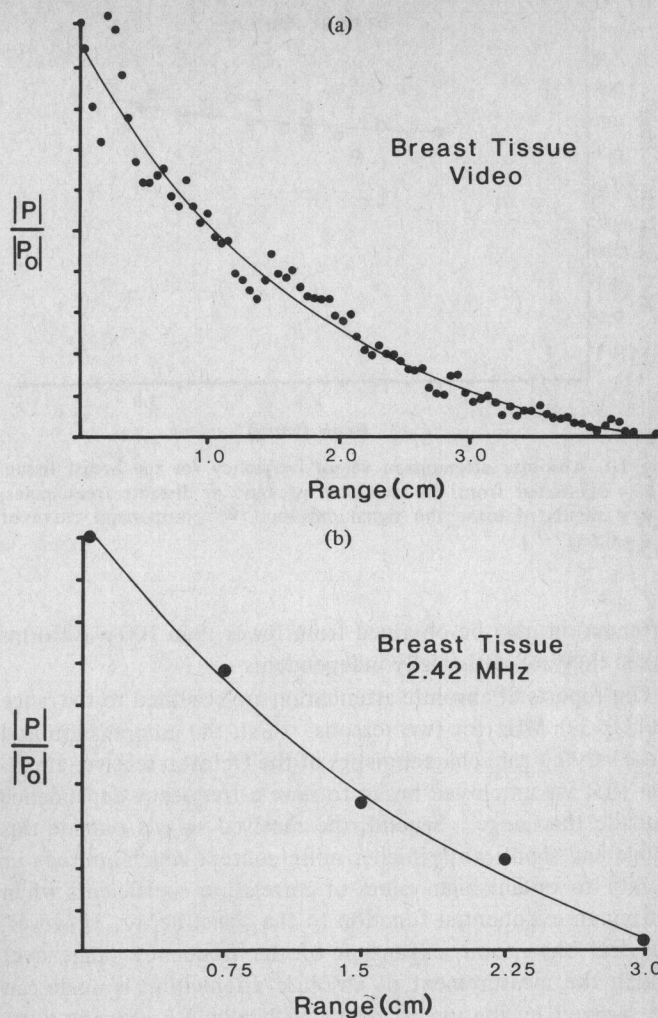


Fig. 9. Average pressure magnitude versus range in the breast (normalized vertical scale). (a) 2.42 MHz data. (b) Video signal. (● = average pressure magnitude, — = fitted exponential.)

neglected for the same reason were any changes in beamwidth arising from the frequency dependence of attenuation.

There are statistical considerations which support the validity of our measurements. A comparison of pressure versus depth data and fitted exponential curves yielded correlation coefficients of greater than 0.95 at those frequencies between 2 and 3 MHz represented in Figs. 4, 7, and 10. These high values of correlation indicate that the average backscattered pressure magnitudes for specific frequencies as a function of depth are well described by exponential curves over the frequency range for which we report data. Also, these correlation values imply that our mean pressure estimates were close to actual mean values as a result of averaging 100 individual waveforms. The small spread of calculated attenuation values around independent measurements indicates that the overall processing steps, including compensation for compression and time-varying gain effects, produce accurate estimates of frequency-dependent attenuation.

The small lateral movement of the transducer between scan lines creates a degree of dependency between neighboring waveforms. Therefore, we believe that good estimates of

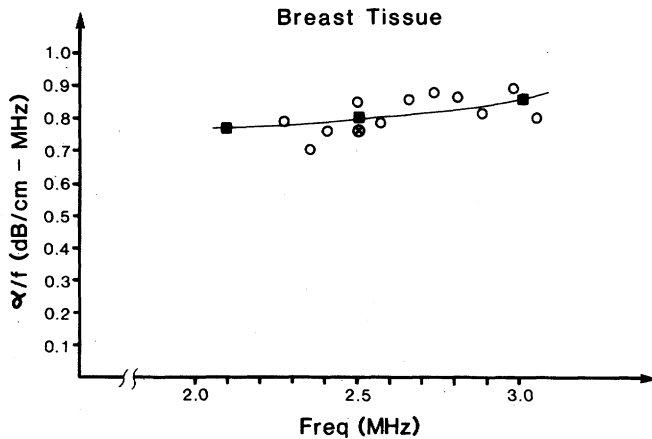


Fig. 10. Absolute attenuation versus frequency for the breast tissue. (O = calculated from the decay of pressure at discrete frequencies, X = calculated using the signal envelope, ■ = comparison curve of $\alpha = 0.61f^{1.3}$.)

attenuation may be obtained from fewer than 100 waveforms when they are statistically independent.

Our reports of absolute attenuation are confined to the range of 2.0–3.0 MHz for two reasons. First, the compression and time-varying gain characteristics of the Octoson receiver amplifier that we employed began to have a frequency dependence outside this range. Second, the received signals outside this range had significantly higher noise content which limited our ability to obtain high values of correlation coefficients when fitting an exponential function to the signal decay. However, we feel that some expansion of the frequency range over which the measurement of absolute attenuation is made can be realized by the use of a broader bandwidth acoustic pulse and receiver amplifier.

The simple approach of calculating the demodulated signal (video as opposed to RF waveform) decay and attributing the resulting attenuation value to the center frequency gave results which were consistent with our other measurements as shown in Figs. 4, 7, and 10. However, use of this method is not strictly justifiable since the broad-band nature of the ultrasonic pulse is ignored. Also, frequency dependence of attenuation cannot be inferred from this single measurement without further assumptions.

A number of issues require further work. The optimal data windowing and segmenting before performing FFT operations must be explored in the analysis of waveforms. The minimum volume of tissue required for accurate measurements needs to be determined. The possible effects of phase distortion by overlying tissue and phase cancellation errors in the receiver remain to be evaluated. Nevertheless, the data reported in this paper show how quantitative attenuation measurements may be incorporated with clinical imaging instrumentation.

CONCLUSION

A mathematical model of ultrasonic scattering has been employed to calculate absolute values of frequency-dependent attenuation from echo signals received by a clinical B-scan imaging system. The model indicates that, after removal of the nonlinear compression and time-varying gain characteristics

of the imaging system, the ensemble average of the pressure magnitude as a function of frequency and tissue depth can be used to derive ultrasonic attenuation. Although additional effort is needed to define the limits of our technique for determining absolute frequency-dependent attenuation, our results from two tissue-mimicking materials and a breast scan are encouraging because of their agreement with independent attenuation measurements.

ACKNOWLEDGMENT

The assistance of Dr. P. Wilson in selecting breast scans for digitization is gratefully acknowledged. The authors are also indebted to Dr. R. Gramiak and Dr. R. Lerner for helpful discussions.

REFERENCES

- [1] P. P. Lele and J. Namery, "A computer-based ultrasonic system for the detection and mapping of myocardial infarcts," in *Proc. San Diego Biomed. Symp.*, 1972, vol. 13, p. 121.
- [2] F. L. Lizzi and D. J. Coleman, "Ultrasonic spectrum analysis in ophthalmology," in *Recent Advances in Ultrasound in Biomedicine*, D. N. White, Ed. Res. Studies Press, 1977, ch. 5.
- [3] M. O'Donnell, J. W. Mimbs, and J. G. Miller, "The relationship between collagen and ultrasonic attenuation in myocardial tissue," *J. Acoust. Soc. Amer.*, vol. 65, pp. 512–517, 1979.
- [4] J. W. Mimbs, M. O'Donnell, J. G. Miller, and B. E. Sobel, "Changes in ultrasonic attenuation indicative of early myocardial ischemic injury," *Amer. J. Physiol.*, vol. 236, no. 2, pp. H340–H344, 1979.
- [5] S. Levi and J. Keuwez, "An attempt to find a differential attenuation coefficient for ultrasonic diagnosis of pelvic tumours in vivo," in *Ultrasound in Medicine*, vol. 3B, *Proc. 1st Triennial Meet. World Fed. for Ultrasound in Med. Biol.*, D. White and R. Brown, Eds. New York: Plenum, 1977, pp. 1989–1993.
- [6] J. F. Greenleaf and R. C. Bahn, "Clinical imaging with transmissive ultrasonic computed tomography," *IEEE Trans. Sonics Ultrason.*, vol. SU-28, pp. 177–185, 1981.
- [7] R. Kuc and M. Schwartz, "Estimating the acoustic attenuation coefficient slope for liver from reflected ultrasound signals," *IEEE Trans. Sonics Ultrason.*, vol. SU-26, pp. 353–362, 1979.
- [8] R. C. Kuc, "Clinical application of an ultrasound attenuation coefficient estimation technique for liver pathology characterization," *IEEE Trans. Biomed. Eng.*, vol. BME-27, no. 6, pp. 313–319, 1980.
- [9] J. C. Bamber and C. R. Hill, "Acoustic properties of normal and cancerous human liver—Dependence on pathological condition," *Ultrasound Med. Biol.*, vol. 7, pp. 121–133, 1981.
- [10] F. L. Lizzi, E. Feleppa, and N. Jaremko, "Liver tissue characterization by digital spectrum and cepstrum analysis," in *Proc. IEEE Ultrasound Symp.*, 1981, pp. 575–578.
- [11] D. A. Sarti and W. F. Sample, *Diagnostic Ultrasound Text and Cases*. Boston, MA: G. K. Hall, 1980, ch. 2.
- [12] P. W. Marcus and E. L. Carstensen, "Problems with absorption measurements of inhomogeneous solids," *J. Acoust. Soc. Amer.*, vol. 58, no. 6, pp. 1334–1335, 1976.
- [13] K. J. Parker, "Attenuation and absorption in liver tissue," *Ultrasound Med. Biol.*, to be published, 1983.
- [14] L. Frizzell, E. Carstensen, and J. Davis, "Ultrasonic absorption in liver tissue," *J. Acoust. Soc. Amer.*, vol. 65, no. 5, pp. 1309–1312, 1979.
- [15] S. A. Goss *et al.*, *Ultrasonic Propagation Parameter Measurements, Ultrasonic Tissue Characterization II*, M. Linzer, Ed. Nat. Bur. Stand., Washington, DC, Special Pub. 525, pp. 43–51, 1979.
- [16] P. M. Gammell, D. H. Le Croissette, and R. C. Heyser, "Temperature and frequency dependence of ultrasonic attenuation in selected tissues," *Ultrasound Med. Biol.*, vol. 5, pp. 269–277, 1979.
- [17] C. R. Meyer, "An iterative, parametric spectral estimation technique for high resolution pulse echo ultrasound," *IEEE Trans. Sonics Ultrason.*, vol. SU-26, pp. 207–212, 1979.

- [18] —, "Preliminary results on a system for wide-band reflection-mode ultrasonic attenuation imaging," *IEEE Trans. Sonics Ultrason.*, vol. SU-29, pp. 12-17, 1982.
- [19] P. M. Morse and K. U. Ingard, *Theoretical Acoustics*. New York: McGraw-Hill, 1968, ch. 8.
- [20] R. C. Waag, R. M. Lerner, and R. Gramiak, "Swept-frequency ultrasonic determination of tissue macrostructure," in *Ultrasonic Tissue Characterization I*, M. Linzer, Ed. Nat. Bur. Stand., Washington, DC, Spec. Pub. 453, pp. 213-228, 1975.
- [21] R. C. Waag, R. M. Lerner, P.P.K. Lee, and R. Gramiak, "Ultrasonic diffraction characterization of tissue," in *Ultrasound in Biomedicine*, vol. I, *Tissue Characterization and New Imaging Techniques*, D. N. White, Ed. Forest Grove, OR: Res. Studies Press, 1978, pp. 87-116.
- [22] R. C. Waag, P.P.K. Lee, H. W. Persson, E. A. Schenk, and R. Gramiak, "Frequency dependent angle scattering of ultrasound by liver," *J. Acoust. Soc. Amer.*, vol. 72, pp. 343-352, 1982.
- [23] W. Clayman, ATS Labs, Norwalk, CT.
- [24] J. Ophir, N. Maklad, and P. Jaeger, "Ultrasound phantom," U.S. Patent 4 286 455, issued Sept. 1, 1981.
- [25] J. Ophir, personal communication, 1982.
- [26] S. A. Goss, R. L. Johnston, and F. Dunn, "Comprehensive compilation of empirical ultrasonic properties of mammalian tissues," *J. Acoust. Soc. Amer.*, vol. 64, pp. 423-457, 1978.
- [27] A. D. Pierce, *Acoustics, An Introduction to its Physical Principles and Applications*. New York: McGraw-Hill, 1981, ch. 10.



Kevin J. Parker (S'79-M'81) was born in Rochester, NY, in 1954. He received the B.S. degree in engineering science from the State University of New York at Buffalo, in 1976 and the M.S. and Ph.D. degrees in electrical engineering from the Massachusetts Institute of Technology, Cambridge, in 1978 and 1981, respectively, with doctoral research on ultrasonic hyperthermia performed at the Laboratory for Medical Ultrasound.

Since joining the faculty at the University of Rochester, Rochester, NY, his research activities have concentrated on tissue characterization using ultrasound.

Dr. Parker is a member of the Acoustical Society of America.

Robert C. Waag (S'59-M'66), for a photograph and biography, see this issue, p. 430.